

Pauline Thompson · Simon L. Harley
Damian P. Carrington

The distribution of H₂O–CO₂ between cordierite and granitic melt under fluid-saturated conditions at 5 kbar and 900 °C

Received: 29 September 2000 / Accepted: 28 April 2001 / Published online: 18 July 2001
© Springer-Verlag 2001

Abstract Experiments to determine the distribution of H₂O and CO₂ between synthetic peraluminous granitic melt and natural Fe–Mg cordierite have been conducted at 5 kbar and 900 °C under fluid-saturated conditions. Up to seven charges, saturated with a range of H₂O–CO₂ fluid compositions, were run simultaneously. The H₂O and CO₂ contents of the cordierites and the H₂O contents of the melts were determined using secondary ion mass spectrometry. As the CO₂ content of the fluid increases, the H₂O content of both the cordierite and the melt decrease in a similar manner to fluid-undersaturated experiments in the H₂O only system. The cordierite H₂O contents in the experiments range from 0.5 to 1.7 wt% H₂O. The distribution coefficients ($D_w = \text{wt\% H}_2\text{O}^{\text{(melt)}} / \text{wt\% H}_2\text{O}^{\text{(cordierite)}}$) are in the range 3.5–5.9 and agree with the model of Harley and Carrington for 5 kbar and 900 °C. The CO₂ content of the cordierite increases from 0 to 1 wt% CO₂ in the most CO₂-rich experiment as the cordierite and melt H₂O contents decrease. Our H₂O–CO₂ cordierite data allow us to model and predict the maximum CO₂ content in cordierite to be 0.16 ± 0.01 molecules per formula unit (i.e. 1.16 wt% CO₂) at 5 kbar and 900 °C. This value, and the channel CO₂ contents of cordierite in equilibrium with H₂O–CO₂ fluids at high XCO₂, are significantly lower than predicted using previous models. On the basis of these experiments cordierites that are saturated in H₂O + CO₂ and have channel XCO₂ > 0.25 require $a\text{CO}_2$ of over 0.75.

Introduction

It is widely recognised that fluids and melts play important roles in the formation and evolution of mineral assemblages during and following high-grade metamorphism in the deep crust. The formation of granulites, migmatites and granites in high-grade terranes may reflect the relative significance of fluid infiltration (e.g. Newton et al. 1980; Santosh et al. 1990; Schmulovich and Graham 1996) compared with melt-present but fluid-absent conditions during metamorphism (Waters and Whales 1984; Barbey et al. 1990; Stevens and Clemens 1993; Watt and Harley 1993) and, as a consequence, it is essential to constrain and elucidate the fluid regime of high-grade metamorphism using a range of complementary approaches.

In order to discriminate fluid-present from fluid-deficient (and often melt-present) conditions, mineral monitors of fluid conditions are required that can complement the isotopic, reaction-progress and mineral equilibria approaches commonly employed to evaluate the extents of fluid interaction and activities of fluid species. Cordierite, $(\text{Mg, Fe})_2\text{Al}_4\text{Si}_5\text{O}_{18} \cdot (n\text{H}_2\text{O, } m\text{CO}_2)$, is potentially a powerful mineral monitor as it incorporates both H₂O and CO₂ within its channel structure and hence can constrain H₂O and CO₂ contents in any coexisting fluid or melt (Goldman et al. 1977; Armbruster and Bloss 1980, 1982; Johannes and Schreyer 1981; Kurepin 1984; Schreyer 1985; Vry et al. 1990). In fluid-present metamorphic environments the absolute abundance and XCO₂ [$= \text{CO}_2 / (\text{CO}_2 + \text{H}_2\text{O})$] of channel volatiles in cordierite depends on pressure, temperature and XCO₂ in the coexisting fluid (Johannes and Schreyer 1981; Armbruster and Bloss 1982). However, in environments where a free volatile phase is not present but temperatures are high (> 750–800 °C; e.g. Vielzeuf and Holloway 1988), the absolute abundance of these channel volatiles may instead depend upon partitioning of H₂O and CO₂ between the cordierite and melt (Harley 1994; Stevens et al. 1995; Carrington and Harley 1996).

P. Thompson (✉) · S.L. Harley
Department of Geology and Geophysics,
University of Edinburgh, Kings Buildings,
West Mains Road, Edinburgh EH9 3JW, UK
E-mail: pauline.thompson@glg.ed.ac.uk
Fax: +44-131-6683184

D.P. Carrington
Online News Editor, *New Scientist*,
151 Wardour St, London W1F 8WE, UK

Editorial responsibility: I. Parsons

Characterisation of the channel volatiles in cordierite formed under known P–T conditions therefore has the potential to discriminate between fluid-present, fluid-absent and melt-present conditions and allow estimation of fluid activities in metamorphism.

The objective of the present experimental study is to determine how the H₂O and CO₂ contents of cordierite vary with the volatile composition of the coexisting fluids and/or melts at 5 kbar and 900 °C. The results define the hitherto poorly-constrained cordierite volatile saturation surface (Johannes and Schreyer 1981; Kurepin 1984; Vry et al. 1990) and demonstrate that the previous modelling of volatile saturation data requires major modification. The saturation data obtained enable cordierite to be used as a monitor of the water contents of the melts that were present during crustal anatexis, as an indicator of the H₂O–CO₂ compositions of fluids that interacted with rocks during their metamorphism, and as a sensor of fluid activities.

Existing data on H₂O–CO₂ contents of cordierite and melts

Volatile contents in cordierite

The maximum volatile contents of cordierite coexisting with pure H₂O have been experimentally calibrated and modelled over the P–T range 1–9 kbar 500–1,000 °C by Harley and Carrington (2001) based on their experiments on Fe–Mg cordierite at 800–1,000 °C and previous experiments on Mg-, Fe- and Fe–Mg cordierite at lower-T (Mirwald and Schreyer 1977; Mirwald et al. 1979; Boberski and Schreyer 1990; Mukhopadhyay and Holdaway 1994; Carey 1995; Skippen and Gunter 1996). Maximum H₂O channel occupancies fit a one-site model (Harley and Carrington 2001) that is compatible with the internally-consistent data set of Holland and Powell (1998).

The situation for the H₂O–CO₂ system is far more uncertain. Experimental data by Johannes and Schreyer (1981) and Armbruster and Bloss (1982) define maximum volatile contents (i.e. the saturation surface of Mg-cordierite in the presence of H₂O–CO₂ and CO₂ respectively) that are mutually inconsistent. Johannes and Schreyer (1981) found that CO₂ contents at 5 kbar and 600 °C differed significantly between different synthetic starting materials, possibly dependent upon the presence of alkali cations in the channels (Johannes and Schreyer 1981; Schreyer 1985). Their cordierite A, an alkali-free synthetic cordierite, showed a trend of increasing CO₂ content that was scattered at higher CO₂/CO₂ + H₂O ratios. Johannes and Schreyer (1981) also presented the results for another synthetic cordierite (B) that showed considerably lower CO₂ contents for a specified fluid composition, but with a much less scattered trend. The CO₂ content in the H₂O-free system determined by Armbruster and Bloss (1982) at equivalent pressures was very high even by comparison

with the trend from cordierite A of Johannes and Schreyer (1981).

The effects of P, T and XCO₂ on cordierite volatile contents have been modelled (Vry et al. 1990) to produce saturation surfaces which are the basis for comparison of analytical data on natural cordierites with predictions from experiments. This saturation surface modelling is, however, simplistic and largely based on the cordierite A volatile content data obtained by Johannes and Schreyer (1981) coupled with the CO₂-system result of Armbruster and Bloss (1982). Kurepin (1984) modelled the saturation surfaces of H₂O–CO₂ fluids in cordierite at polybaric and polythermal conditions assuming a one-site model with a fit to the H₂O solubility data from the water-only system (Mirwald et al. 1979) and a model of H₂O–CO₂ behaviour in cordierite that approximates the cordierite A data of Johannes and Schreyer (1981). Cordierite B fitted this model at lower pressures and higher water contents at 600 °C but otherwise the CO₂ contents were significantly lower than those predicted by the Kurepin (1984) model. The fit of both the cordierite A and B data also appear to deteriorate at the temperature extremes, but nevertheless the Kurepin (1984) model has been used extensively in later applications and is applied in the internally-consistent data set approach of Holland and Powell (1998) despite its shortcomings.

Further attempts at defining the saturation contents of CO₂ in cordierite in the H₂O-free system have been largely unsuccessful, and moreover have failed to duplicate the early result of Armbruster and Bloss (1982). Le Breton and Schreyer (1993) could not equilibrate natural and synthetic cordierites with CO₂ fluid in their experiments carried out at 8–12 kbar and 600–800 °C in piston cylinder (solid media) apparatus. These workers found that CO₂ contents varied with experimental run duration, and in particular documented oscillations in CO₂ with time. There is no completely satisfactory explanation of this behaviour.

In this study we adopted a three-phase experimental design to minimise problems of volatile equilibration in cordierite. Each experiment contains cordierite, melt and a coexisting H₂O–CO₂ fluid phase. H₂O is strongly incorporated into the melt and cordierite and the fluid XCO₂ can be varied to high values at specified P–T conditions. The presence of melt with cordierite provides limits on post-run volatile adjustments in cordierite as melt–cordierite contacts become ‘locked’ at the quench temperature of the melt. Moreover, both cordierite and melt can be used as monitors of the H₂O activity of the experiment (Harley and Carrington 2001) and hence the approach to equilibrium.

Volatiles in felsic and peraluminous melts

The maximum solubilities of H₂O in eutectic melts within various simplified granitic systems are now well-defined from several studies (e.g. Holtz et al. 1992; Holtz

and Johannes 1994; Papale 1997). The maximum solubility of CO₂ in rhyolitic melts, although low at mid-crustal pressures (<4,000 ppm) is strongly pressure-sensitive (Fogel and Rutherford 1990; Blank and Brooker 1994; Holloway and Blank 1994). In contrast to the large database now available for H₂O, the combined solubilities of H₂O and CO₂ in felsic melts in a mixed volatile system are poorly known at pressures greater than 2 kbar, even though such pressure conditions (2–8 kbar) are highly relevant to the generation and segregation of many crustally-derived magmas. The present study also explores the variation in the H₂O content of a granitic melt with differing fluid compositions at 5 kbar and 900 °C. The variation in melt CO₂ contents were too small to detect with appropriate levels of precision using secondary ion mass spectrometry, but the small quantity of CO₂ (probably <1,000 ppm) can be demonstrated to have negligible effect on the behaviour of H₂O in the melt.

Experimental design

The presence of a melt along with cordierite and fluid has three advantages compared with simple experiments that attempt to equilibrate cordierite with only a mixed H₂O–CO₂ fluid phase:

1. The melt provides a reservoir for H₂O that effectively ‘quenches in’ at high temperatures (>650–750 °C) and hence causes the experiment to ‘lock-in’ soon after power is cut off. This limits the opportunity for low-temperature Crd–fluid exchange, which could modify the cordierite H₂O–CO₂ contents from those of the run conditions, to progress at intact cordierite–melt contacts. There are very few fluid bubbles present at Crd–melt contacts in these experiments, so that a large fluid reservoir is not available to exchange with the cordierite once the melt has solidified.
2. The approach to equilibrium can be judged, at least for H₂O contents, by comparing measured distribution coefficients ($D_W = \text{wt}\% \text{H}_2\text{O}^{(\text{melt})} / \text{wt}\% \text{H}_2\text{O}^{(\text{cordierite})}$) with those predicted from the models of Harley and Carrington (2001) in the H₂O-only system, governed by equilibria (1) and (4) below.
3. $a_{\text{H}_2\text{O}}$ (and from this, a_{CO_2}) can be calculated from both cordierite and melt, albeit with differing uncertainty limits depending on the homogeneity of the run products. Hence, in experiments where the cordierite H₂O data are subject to high relative analytical errors, the melt H₂O data can provide more precise $a_{\text{H}_2\text{O}}$ estimates for defining the relations between a_{CO_2} and $X_{\text{CO}_2(\text{Crd})}$.

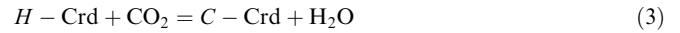
Experimental charges comprised cordierite (Crd), granitic melt (*L*) and an H₂O–CO₂ fluid (*V*). In this system the following equilibrium relationships describe the uptake of H₂O and CO₂ in cordierite:



and

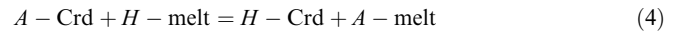


which are linked by the exchange relationship:

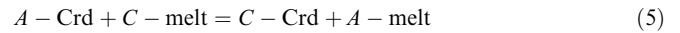


where *A*-Crd is volatile-free cordierite, *H*-Crd is hydrous cordierite (Crd.H₂O, with H₂O up to a maximum of one molecule per formula unit of cordierite) and *C*-Crd is Crd.CO₂, with CO₂ up to a maximum of one molecule per formula unit.

Furthermore, exchange equilibria for H₂O and CO₂ apply between the cordierite and granitic melt:



and



As demonstrated in previous studies in the H₂O-only subsystem, the Fe–Mg composition of cordierite does not have a measurable effect on the molecules per formula unit of volatile incorporated in the phase at a given *P*–*T* and $a_{\text{H}_2\text{O}}$ (Boberski and Schreyer 1990; Carrington and Harley 1996; Harley and Carrington 2001). A natural cordierite, BB3a, with $X_{\text{Mg}} = 0.66$ (Table 1) was used once it had been crushed and sieved to 125–250 μm. This cordierite had been evacuated of all volatiles prior to the experiment by prolonged step-heating in a high vacuum at temperatures of up to 1,200 °C. In this evacuation procedure the cordierite is held for 1 h at each 100 °C temperature step below 1,200 °C, for 2 h at 1,200 °C, and heated for a minimum of 12 h in total. The vast proportion of CO₂ is liberated from the cordierite channels only at temperatures over 800 °C, and often at above 1,000 °C. The granitic melt was introduced into the experiments in the form of a K₂O–Na₂O–FeO–MgO–Al₂O₃–SiO₂ system gel ($X_{\text{Mg}} = 0.25$, Table 1) and chosen to be close to Fe/Mg equilibrium with the cordierite (Carrington and Harley 1995). Different fluid compositions were generated in different charges by adding carefully measured quantities of distilled H₂O (using a microsyringe), silver oxalate (Ag₂C₂O₄ decomposes to release 29.0 wt% CO₂) and oxalic acid [(COOH)₂.2H₂O decomposes to release 69.8 wt% CO₂ and 28.6 wt% H₂O]. Table 2 gives the proportions of starting materials in each run. The experiments were performed at 5 kbar and 900 °C in an internally heated gas apparatus that has pressure and temperature uncertainties of ±0.2 kbar and ±5 °C, respectively (Carrington and Harley 1995). Up to seven charges with differing fluid compositions could be run in one operation for between 137 and 524 h. Tantalum chips were placed outside the capsules to moderate the f_{O_2} and prevent loss of hydrogen from the capsule fluids. At the end of the experiment the charges were weighed, pierced

Table 1 Experimental starting materials and SIMS standards: mean electron microprobe analyses ($n = 6$). Melt data has been normalised to ease comparison

	Starting materials		Standards	
	BB3a	81–90	AMNH	
SiO ₂	48.12	47.70	48.70	
Al ₂ O ₃	33.02	32.72	33.16	
FeO	8.61	6.19	2.58	
MgO	8.57	9.74	12.24	
K ₂ O	0.03	0.11	0.39	
Na ₂ O	0.05	0.01	0.01	
H ₂ O ^a		0.80	1.54	
CO ₂		1.3 ^b	0.7 ^c	
Total	98.42	97.29	98.63	
X _{Mg}	0.64	0.74	0.89	
	Melt gel		Glass standards	
SiO ₂	73.57	74.46	75.78	76.43
Al ₂ O ₃	15.05	16.46	15.89	15.94
FeO	1.82	0.70	0.59	0.72
MgO	0.40	0.15	0.13	0.14
K ₂ O	4.79	3.36	2.66	1.94
Na ₂ O	4.37	4.26	4.35	4.24
H ₂ O ^d		2.1	3.9	5.6
Total	100.00	100.00	100.00	100.00
X _{Mg}	0.28	0.28	0.28	0.25

^aBy hydrogen extraction and manometry (A. Fallick)^bBy coulometric titration (V. Schenk)^cBy stepped-heating mass spectrometry (D. Matthey)^dKarl–Fisher titration (F. Holtz)**Table 2** Starting materials, run durations and SIMS analyses of the H₂O and CO₂ contents of cordierites and melts for all experiments used in this study. SIMS errors given in brackets are 1σ values propagated from variations in the analysis populations ($n = 8–10$). No data = not included in charge

	Starting materials					Experimental results			
	H ₂ O (g)	Oxalic acid (g)	Silver oxalate (g)	Cordierite (g)	Melt gel (g)	Time (h)	Cordierite wt% H ₂ O	Cordierite wt% CO ₂	Melt wt% H ₂ O
C13-1 (–)	2.84	–	2.51	3.02	7.08	137	2.03 (0.09)	0.26 (0.05)	8.57 (0.37)
C13-2 (–)	2.21	–	4.16	2.48	7.15	137	1.73 (0.08)	0.29 (0.01)	8.23 (0.82)
C13-3 (–)	1.52	–	5.06	2.25	6.93	137	1.59 (0.07)	0.44 (0.04)	6.97 (0.54)
C13-4 (–)	–	3.94	3.89	2.83	7.11	144	1.33 (0.07)	0.64 (0.07)	5.49 (0.28)
C13-5 (–)	–	2.03	5.13	3.01	7.86	144	1.09 (0.07)	0.80 (0.06)	3.86 (0.28)
C19-4 (–)	0.30	–	2.44	2.78	6.48	238	0.57 (0.03)	1.01 (0.14)	Crystallised
C19-3b (–)	0.33	–	2.18	2.66	6.61	524	0.64 (0.08)	1.03 (0.17)	Crystallised
C20-1 (–)	0.45	–	2.08	2.56	5.61	173	1.37 (0.14)	0.53 (0.05)	6.03 (0.68)
C13-1 (+)	2.84	–	2.51	3.02	7.08	137	1.55 (0.07)	0.26 (0.05)	8.57 (0.37)
C13-5 (+)	–	2.03	5.13	3.01	7.86	144	0.92 (0.04)	0.80 (0.06)	3.86 (0.28)
MP13B (+) ^a	1.28	–	–	2.56	6.56	311	1.70 (0.05)	0.00 (0.00)	10.02 (0.42)
H ₂ O model ^a							1.76	0.00	10.20

^aData from Harley and Carrington (2001)

and reweighed to check for capsule integrity during the experiment. They were then vacuum impregnated with epoxy resin, mounted and polished until a section through the cordierite grains and melt was observed.

Characterisation and analysis of run products

Initially, the polished charges were examined optically for the presence of fluid inclusions in the melt. Fluid-saturated experiments contain a free fluid during the experiment that may be trapped as bubbles in the melt on quenching. Cordierite and melt were the only run products in most cases, but at low H₂O contents

(<2.2 wt% H₂O) the melts partially or completely crystallised to quartz and feldspar, as is expected from their near-eutectic compositions. In the two most H₂O-rich experiments cordierite showed minor resorption producing fine grains of spinel located at cordierite–melt contacts.

The H₂O and CO₂ contents of the experimental cordierite and melt were analysed using secondary ion mass spectrometry (SIMS). All other oxides were measured with a wavelength-dispersive electron microprobe (EMP) in Edinburgh and compared with data from the energy-dispersive scanning electron microscope (SEM) using a cold stage in Manchester. The analytical conditions used for EMP were the same as those detailed in

Carrington and Harley (1996) and Harley and Carrington (2001). Calibration curves were obtained in each SIMS session by analysis of melts and cordierites of appropriate compositions, but differing volatile contents that had been independently determined (Table 1). The three melt standards contained 2.1, 3.9 and 5.6 wt% H₂O (provided by Dr F.R. Holtz). Melts with higher H₂O contents (up to 10 wt%, the approximate saturation content at 5 kbar and 900 °C) were synthesised, but were unstable over long time periods at room pressure and temperature. The two cordierite standards contained 1.56 (AMNH) and 0.86 (81/90) wt% H₂O and 0.66 (AMNH) and 1.30 (81/90) wt% CO₂, respectively. All melt analyses and a subset of the cordierite analyses were obtained using an O⁻ primary beam (8 nA, 10 kV) and by measuring positive secondary ions (H⁺, ³⁰Si) at an energy offset of 75 V. Cordierites were also analysed using negative secondary ions (H⁻, ¹²C and ²⁸Si) at an energy offset of 60 V. The sputtered pit in the sample is roughly 25 µm in diameter in the positive mode and 35 µm in the negative mode. Each analysis involves a 3-min burn-in time followed by 30 cycles of 5-s counts for each isotope. The mean of the isotope ratios of the last 10 cycles was taken as the final result, thereby avoiding surface contamination. Analyses were expressed as isotopic ratios of H⁺/³⁰Si (positive mode) or H⁻/²⁸Si and ¹²C/²⁸Si (negative mode) and then converted to wt% H₂O or CO₂ by comparison with the calibration lines from the standards from the same analytical session. Standard errors on analytical populations for individual standard melt and cordierite grains with positive secondary ions were typically ±0.8 and ±0.2 wt% H₂O, respectively, yielding calibration curves with 2 sigma uncertainties of 0.15 and 0.06 wt% H₂O for melt and cordierite H₂O contents of 3 and 1 wt% H₂O, respectively. Equivalent standard errors on analytical populations for individual standard cordierite grains measured with negative secondary ions were ±0.16 wt% H₂O and ±0.08 wt% CO₂. Calibration curves for negative secondary ions thus had 2 sigma uncertainties of 0.12 wt% H₂O and 0.06 wt% CO₂ for 1 wt% H₂O and 1 wt% CO₂ in the cordierite, respectively.

Difficulties were encountered in measuring the low CO₂ contents (<1,000 ppm) in melt standards and hence also in the experimental granitic melts, which appear to contain less than 1,000 ppm CO₂, that form in equilibrium with cordierite of moderate CO₂ content (<1 wt%) and are significantly lower than the maximum CO₂ contents (~2,600 ppm) in rhyolite glass at 900 °C (Holloway and Blank 1994). The glass standards were mounted in indium metal to minimise the carbon background resulting from any epoxy resin. Despite this, the measured ¹²C/²⁸Si ratios for glasses synthesised nominally without CO₂ were indistinguishable from those measured for a glass characterised by FTIR spectroscopy (Bristol) to have 300 ppm CO₂. To further reduce the presumed high carbon background, a 50-nA primary beam was rastered over 50 µm and the counts measured through a 10-µm aperture, but the sum of the

counts from background carbon and from any CO₂ in the 'blank' glasses was still at least 300 ppm. In view of these problems we concentrated on obtaining H₂O analyses on the melts (positive mode) and H₂O–CO₂ on the cordierites (negative mode CO₂; positive and negative mode for H₂O).

Experimental results

Phase chemistry

Melts

The melt composition was chosen to be in Fe/Mg equilibrium with the cordierite and close to the eutectic minimum melt composition (Carrington and Harley 1996). The oxide contents of the final experimental glasses were analysed using the electron microprobe. The lack of a cold stage on the electron microprobe caused significant volatilisation of the sodium. These 5 kbar, 900 °C samples were all mounted in indium and could not be thinned for analysis on the analytical SEM cold stage in Manchester. However, the data could be corrected for sodium loss by comparison with both EMP and SEM data from similar experiments at other pressure–temperature conditions. These comparisons indicate that the glasses did not change significantly from the minimum melt composition in any of the experiments and were in close agreement with the data for the water-undersaturated system of Harley and Carrington (2001). Thus the presence of CO₂ in the system, and hence in the melt, does not appear to change the melt compositions significantly. This is important in respect of controversy regarding the stabilisation of lamprophyric melt compositions in felsic systems, as proposed by Petersen and Newton (1990) and disputed by Clemens (1993) and others. Our results reconfirm the conclusions of Clemens (1993) that CO₂ does not enhance melting and certainly does not shift melt compositions to high-K, low-Si compositions.

Cordierites

Product cordierite compositions demonstrate the same effects as that seen in the H₂O experiments of Harley and Carrington (2001). Occasionally some cordierites showed minor near-rim shifts in X_{Mg}, usually to slightly higher X_{Mg} as indicated by back scattered electron brightness changes. Apart from these rims, systematic analyses of cordierite compositions are very consistent. Only potassium varies, by less than 0.2 wt% K₂O. The potassium content increases with temperature and decreases with water content, as reported in Thompson et al. (2001).

Fluids

All experiments contained a free fluid phase during the run, as shown by capsules emitting gas when pierced and

by weight loss. Polished surfaces showed sections through bubbles in the melt phase. These fluids were not analysed after the experiments. The initial proportions in Table 2 can be used to calculate the initial fluid composition and estimate the final fluid compositions by mass balance. However, such estimates may involve several sources of error and hence are less reliable for activity calculations than the methods we use below. Potentially important sources of error include inaccuracies in capsule manufacture, small changes in the proportions of the phases during the experiments (e.g. because of reaction) and cumulative uncertainties on the measured volatile contents of the phases. The unquantified CO₂ contents of the experimental melts have a negligible effect on the mass balance calculations; a maximum CO₂ content of 2,600 ppm (Holloway and Blank 1994) would only change our fluid XCO₂ estimates by less than 0.2%. Our mass balance calculations (not tabulated) are generally consistent with the estimates of fluid XCO₂ produced using the approach adopted here (see later section). However, as they show significantly greater scatter in estimated XCO₂ they are not used in further calculations.

Time study – approach to equilibrium

In the H₂O experiments at 5 kbar and 900 °C of Harley and Carrington (2001) sandwich-type charges showed that the values of D_w [=wt% H₂O^(melt)/wt% H₂O^(cordierite)] of initially evacuated cordierite at one end and fully saturated cordierite at the other approached each other with 24 h. The presence of CO₂ may affect the diffusion of volatiles in the cordierite and hence a time study was conducted to evaluate the approach to equilibrium in CO₂-rich compositions. Four charges were made with similar bulk initial proportions of 2.9 ± 0.3 wt% H₂O, 6.5 ± 0.4 wt% CO₂, 25.6 ± 1.5 wt% evacuated cordierite and 64.9 ± 1.8 wt% gel. These four charges were then run for different durations. The final compositions of these experiments are shown in Table 3. After 119 h, the volatile compositions of the cordierites agree within error implying that equilibrium of the cordierite volatile composition has been achieved. Equilibrium conditions are thus likely to have occurred in all further experiments that were run for 137–422 h.

Water contents of melts and cordierites

The results of SIMS analyses of the run products of all the H₂O–CO₂ data are listed in Table 2. Figure 1 is a plot of wt% of volatiles (H₂O or CO₂) in the cordierite against the wt% of H₂O in the melt from the same experiment. The H₂O contents in both the cordierite and melt decrease from their maximum values (1.78 and 10.20 wt% H₂O respectively in the pure water system) as the CO₂ in the cordierite increases.

The H₂O in the cordierites in two of the run products (C13-1 and C13-5) were measured with both positive (Fig. 1, open squares) and negative (Fig. 1, closed squares) secondary ions but all others were measured in negative mode alone. In our larger data set of cordierite–melt experiments, run over a range of P–T conditions, we have made 22 positive/negative comparisons. Of these 17 showed very close agreement between the values in both modes. However, two showed a slightly higher value in positives and two, C13-1 and C13-5 reported here, had significantly lower values in positives than negatives. C13-1, the most hydrous of the H₂O–CO₂ experiments, has a large difference between the cordierite water content measured in positive and negative mode. C13-5 shows that the difference is small at lower water contents. SIMS analyses of natural cordierites have also been compared in positives and negatives and no such sizeable discrepancies have been found. The reason for these occasional differences is not apparent, but in the light of all other experiments the values measured in positives appear more consistent and thus these are preferred in those cases where +/- discrepancies were

Table 3 Results of a time study to determine how long it takes to reach constant volatile content in cordierite with a CO₂-rich fluid. Starting materials are given in Tables 1 and 2

Run	Duration (h)	Cordierite (wt% H ₂ O)	Cordierite (wt% CO ₂)	XCO ₂ in Crd Channels
c19-1	24	0.84 (0.08)	0.88 (0.11)	0.30 (0.05)
c19-2	119	0.54 (0.03)	1.21 (0.16)	0.48 (0.08)
c19-4	238	0.57 (0.03)	1.01 (0.14)	0.42 (0.07)
c19-3b	524	0.64 (0.08)	1.03 (0.17)	0.40 (0.08)

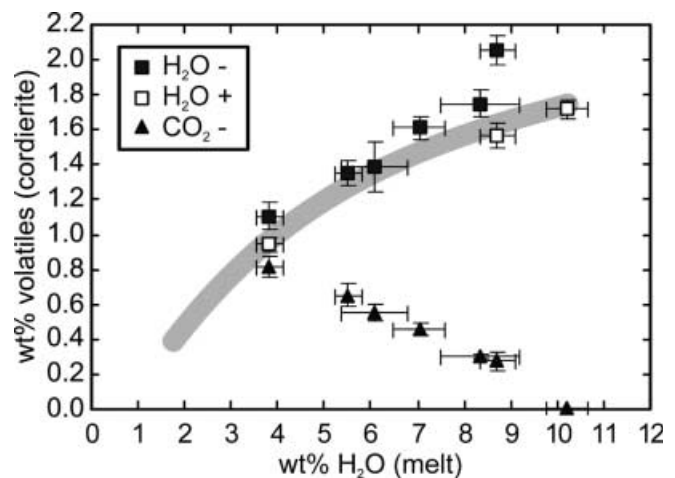


Fig. 1 A graph showing the volatile contents in the cordierite at 5 kbar, 900 °C as a function of the water content of the melt. Squares H₂O contents; triangles CO₂ contents; closed symbols H₂O measured in negative mode; open symbols H₂O contents measured in positive mode. The thick line is the trend of H₂O content (including errors) taken from Harley and Carrington (2001) for undersaturation in the water-only system. This trend reaches saturation at 1.76 and 10.20 wt% H₂O for cordierite and melt, respectively

found. The anomalous values in negatives may be a problem associated with that particular analysis session and thus all the other cordierite H₂O values for C13 may be slightly high.

The decrease in H₂O content of the cordierite with decreasing melt water content (Fig. 1) in these CO₂-bearing fluid-saturated experiments closely follows the behaviour of H₂O-undersaturated cordierites observed by Carrington and Harley (1996). Only C13-1 measured in negatives has an anomalously high value. The points measured in negatives all lie within error but on the high side of the trend shown by the water-only data whereas those in positive mode lie on the low side. Overall, the H₂O–CO₂ trend brackets and is indistinguishable within error from the H₂O-undersaturated trend defined by Harley and Carrington (2001), which is shown as a broad curve on Fig. 1.

The distribution coefficient [$D_w = \text{wt}\% \text{H}_2\text{O}^{(\text{melt})} / \text{wt}\% \text{H}_2\text{O}^{(\text{cordierite})}$] of H₂O between melt and cordierite is plotted in Fig. 2. The broad curve in Fig. 2 is taken from the model of the water-only system of Harley and Carrington (2001) for 5 kbar and 900 °C. The D_w values for the positive data and all negative data except the anomalous C13-1 (in negative mode) lie within error of this modelled trend. Therefore, the incorporation of CO₂ into cordierite and melt has no additional effect on D_w compared with the simple effect of reduction in $a_{\text{H}_2\text{O}}$. For a melt of specified H₂O content D_w is the same whether the coexisting cordierite contains CO₂ or not.

Relation of CO₂ to water in cordierite

Figure 1 also shows the variation in the CO₂ content of the cordierite. The data all lie on a curve antithetic to the

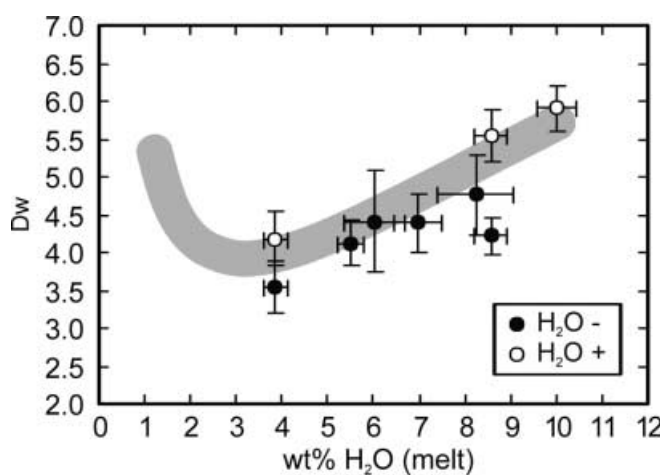


Fig. 2 The relation between the distribution coefficient $D_w = [\text{wt}\% \text{H}_2\text{O}^{(\text{melt})} / \text{wt}\% \text{H}_2\text{O}^{(\text{cordierite})}]$ and the water content of the melt. *Closed symbols* Measured in negatives; *open symbols* measured in positives. The *thick line* shows the model (including errors) of D_w variation with undersaturation in the water-only system (Harley and Carrington 2001) for 5 kbar and 900 °C. This modelled curve terminates at 10.20 wt% H₂O in the melt when H₂O saturation is achieved

curve shown by the variation of the water content in the cordierite. The CO₂ contents range from zero in the hydrous cordierite to 0.8 wt% in the most CO₂-rich experiment of Fig. 2 where the melt is 3.86 wt% H₂O. It is possible to get higher cordierite CO₂ contents, of over 1 wt% CO₂, in experiments C19-4 and C19-3b, but at these conditions the water content of the melt drops below its minimum value [approximately 2 wt% H₂O, Johannes and Holtz (1996) and Carrington and Harley (1996)] and crystallises. The curve of Fig. 2 extrapolates to the CO₂-only end at a maximum value of CO₂ in cordierite of 1.16 wt% CO₂, a value derived by modelling of the data in terms of fluid activities (see below). Under these H₂O-free conditions melt is not stable at 900 °C.

Modelling of activity functions of CO₂ in cordierite at 5 kbar and 900 °C

Key aims of this study were to constrain the uptake of CO₂ in cordierite as a function of a_{CO_2} in the system and hence define the maximum CO₂ content attainable in cordierite at 5 kbar and 900 °C. The latter could not be done directly as our experiments only contained mixed H₂O–CO₂ fluids; experiments with pure CO₂ fluids would have not produced melt at this pressure and temperature. The approach to be used, therefore, is to calculate the maximum cordierite CO₂ content from the experimental data using independently-constrained calibrations of the a - X relations for H₂O in cordierite and melt. This can be accomplished via extrapolation of these a - X relations to the condition where $a_{\text{H}_2\text{O}} = 0$ ($a_{\text{CO}_2} = 1$). From calculated values of $a_{\text{H}_2\text{O}}$ for experimental cordierite-melt pairs at fluid-saturation, a_{CO_2} can be determined by solving the equation of state for H₂O–CO₂ fluid mixing at the P–T of interest, consistent with the Gibbs–Duhem relation. With a_{CO_2} calculated from the phase water contents in this way, the variation of CO₂ in cordierite with a_{CO_2} can be assessed through the adoption of an appropriate volatile incorporation model for cordierite.

Calculation of $a_{\text{H}_2\text{O}}$ and a_{CO_2} from melt and cordierite H₂O data

Following Harley and Carrington (2001), the relationship between $a_{\text{H}_2\text{O}}$ and the solubility of H₂O in relevant granitic melts at a specified P–T condition is closely approximated by the ‘Burnham-type’ model (Burnham and Nekvasil 1986):

$$a_{\text{H}_2\text{O}} = k_w (X_w)^2 \quad \text{for } X_w \leq 0.5 \quad \text{and} \\ a_{\text{H}_2\text{O}} = 0.25k_w [\exp((6.52 - (2667/T)) \cdot X_w)] \quad \text{for } X_w > 0.5 \quad (6)$$

where X_w is the mole fraction of water in a melt calculated with 8-oxygens per formula unit and k_w is a P–T dependent coefficient. In this case k_w is extracted from

the H₂O-system cordierite-melt experiments of Harley and Carrington (2001), rather than calculated from the k_w model expressions of Burnham (1994), as the former were conducted under equivalent P–T conditions and in an analogous compositional system. At 5 kbar and 900 °C, the melt H₂O contents at fluid saturation, measured and modelled in Harley and Carrington (2001: 10.2 wt% H₂O), define k_w to be 2.42.

The maximum H₂O-contents of cordierite coexisting with pure H₂O have now been successfully determined at 3–7 kbar to 1,000 °C. Harley and Carrington (2001) modelled the cordierite saturation hydration data (Mirwald et al. 1979; Boberski and Schreyer 1990; Mukhopadhyay and Holdaway 1994; Carey 1995; Carrington and Harley 1996; Skippen and Gunter 1996; Harley and Carrington, 2001) together with their undersaturation data. This modelling demonstrates that the relation between $a_{\text{H}_2\text{O}}$ and the H₂O content of cordierite, governed by equilibrium (1), can be expressed as

$$a_{\text{H}_2\text{O}} = z_w \cdot [n/(1-n)] \quad (7)$$

where n is the number of molecules of H₂O per formula unit of cordierite, and z_w is a P–T dependent coefficient. At 5 kbar and 900 °C, the H₂O saturation value of n , defined by Harley and Carrington (2001), is 0.6 molecules per formula unit, such that z_w is 0.6667.

Using these values of k_w and z_w and the a -X relations for melt and cordierite respectively, we can produce pairs of calculated $a_{\text{H}_2\text{O}}$ values for each Crd–melt experiment conducted at 5 kbar and 900 °C. Furthermore, a_{CO_2} in the fluid-saturated two-component H₂O–CO₂ system is not independent of $a_{\text{H}_2\text{O}}$, but rather a function of it. Hence, the $a_{\text{H}_2\text{O}}$ pairs can be converted to pairs of a_{CO_2} values pertaining to each experiment, through solution of the Gibbs–Duhem relation and taking non-ideal, P–T dependent fluid-mixing properties into account. In this study we have adopted the asymmetric regular solution approximation to the modified Redlich–Kwong equation of state for H₂O–CO₂ mixing as formulated by Holland and Powell (1990).

Maximum CO₂ content of cordierite

Defining m as the number of molecules of CO₂ per formula unit in cordierite, and using a one molecule per formula unit one-site model, consistent with the hydration model (7) referred to above

$$a_{\text{CO}_2} = z_c [m/(1-m)] \quad (8)$$

where z_c is a P–T sensitive coefficient that is the CO₂-system analogue of z_w . However, unlike the H₂O-system, z_c cannot be calculated directly from data available at unit a_{CO_2} .

In our experiments $m/(1-m)$ is evaluated from the measured cordierite CO₂ data. Hence a plot of $m/(1-m)$ versus a_{CO_2} , calculated as described above from the cordierite or melt H₂O contents, demonstrates a good

linear fit consistent with the predicted relationship between cordierite CO₂ contents and the CO₂ activity (Fig. 3). The best-fit line through the data can be extrapolated to $a_{\text{CO}_2} = 1$ ($a_{\text{H}_2\text{O}} = 0$) in order to evaluate m_{sat} , the saturation number of CO₂ molecules in cordierite in the H₂O-free subsystem. At 5 kbar, 900 °C and $a_{\text{CO}_2} = 1$, m_{sat} is found to be 0.16 ± 0.01 molecules of CO₂ per formula unit of cordierite.

Intermediate H₂O–CO₂ compositions

Once the maximum CO₂ content of cordierite at 5 kbar and 900 °C has been established as shown above a value for z_c can be determined at $a_{\text{CO}_2} = 1$ from

$$z_{c(P,T)} = (1 - m_{\text{sat}})/m_{\text{sat}} \quad (9)$$

Thus, $z_{c(P,T)}$ at 5 kbar and 900 °C is calculated as 5.25, whereas $z_{w(P,T)}$ evaluated previously for this P–T is 0.667. Using these data and the relations (7) and (8), the expressions:

$$\begin{aligned} a_{\text{H}_2\text{O}} &= 0.667 \cdot [n/(1-n)] \\ a_{\text{CO}_2} &= 5.25 \cdot [m/(1-m)] \end{aligned}$$

can be applied to calculate the channel volatile contents (n , m) of cordierite at intermediate fluid compositions (i.e. for compatible $a_{\text{H}_2\text{O}}$ – a_{CO_2} pairs consistent with the non-ideal fluid mixing model). The results of this calculation, shown by the lines in Fig. 4, agree well with the original raw data expressed in terms of m and n .

Comparison with previous experimental work

There are no other complete data sets from previous work at 5 kbar and 900 °C. Johannes and Schreyer

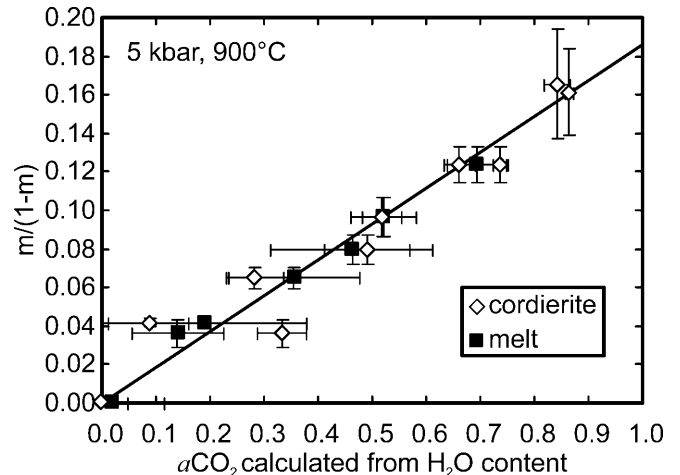


Fig. 3 A plot of the activity function of cordierite as $m/(1-m)$ versus the activity of CO₂ calculated from the $a_{\text{H}_2\text{O}}$ data. The line is the best fit line through the points and its value at $a_{\text{CO}_2} = 1$ allows us to estimate m_{sat} in the H₂O-absent case

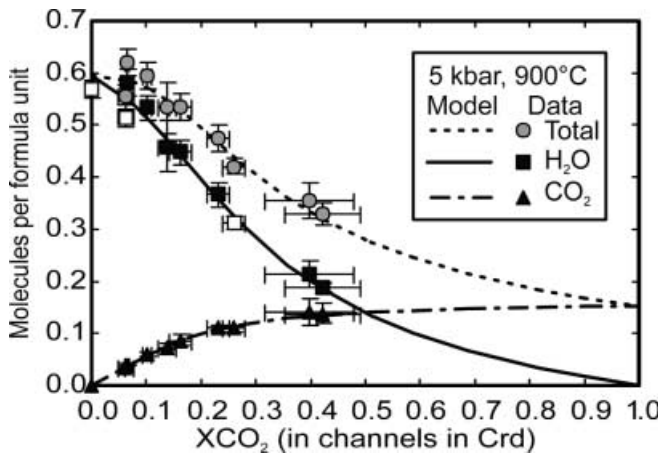


Fig. 4 Variation of the volatile composition in the cordierite channels with fluid-saturated, intermediate composition H₂O–CO₂ fluids. The lines show the modelled values agree well with the original raw data. Closed symbols H₂O measured in negatives; open symbols H₂O measured in positives; triangles CO₂; circles total number of molecules per formula unit

(1981) ran one experiment at 5 kbar and 900 °C, but otherwise the closest full set is their data at 5 kbar and 800 °C on their cordierite B starting material. We have taken these data and estimated the $a\text{CO}_2$ values from the $a\text{H}_2\text{O}$ for their experiments using the methods we applied to our data (described above). The parameter z_w is again derived from the saturation data in the CO₂-free system (Harley and Carrington, 2001). The $a\text{CO}_2$ calculated from the cordierite H₂O content data in Johannes and Schreyer (1981) are plotted against their $m/(1-m)$ for both P–T conditions in Fig. 5. For comparison our best-fit line from Fig. 4 at 5 kbar and 900 °C is also shown on the plot. The equivalent line for 5 kbar and 800 °C should be at slightly higher $m/(1-m)$ values as there is a slight decrease in the CO₂-content of cordierite with increasing temperature (Johannes and Schreyer 1981 Fig. 5). At the higher CO₂ end of the graph Johannes and Schreyer's data points at 5 kbar and 800 °C agree more closely with our predictions. However, at intermediate CO₂ activities their data are significantly CO₂-poor compared with our predicted values. Their data including the 5 kbar 900 °C point do lie on a fairly linear trend, but one with a large negative intercept at $a\text{CO}_2=0$. The scattered 5 kbar, 800 °C data of Johannes and Schreyer is difficult to explain, but may suggest poor attainment of equilibrium, perhaps reflecting slow filling of cordierite channels with CO₂ compared with run duration, or variable re-equilibration on cooling and quenching. The results of our NKFMAH–CO₂ study do not account for chemical variations in any other components in the cordierite channels. This may partly explain the discrepancies found in relation to previous works. Nevertheless, plots such as Fig. 5 demonstrate that the H₂O and CO₂ data reported from the previous experiments are often internally inconsistent and should be treated with caution.

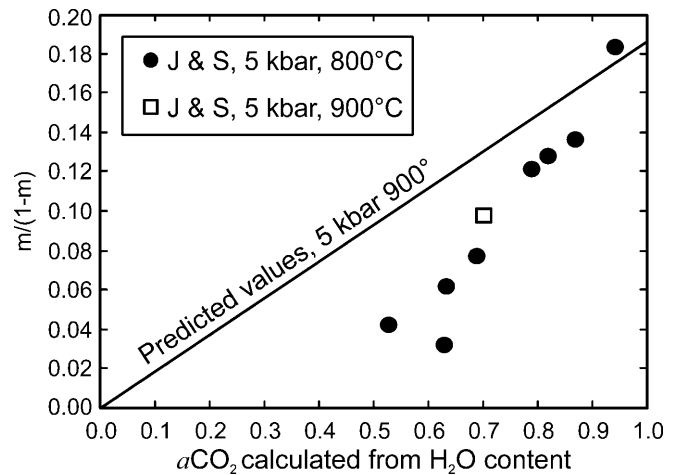


Fig. 5 A plot of $m/(1-m)$ against $a\text{CO}_2$ calculated from the $a\text{H}_2\text{O}$ for the 5 kbar 800 and 900 °C data of Johannes and Schreyer (1981). The line shows our predicted values for 5 kbar and 900 °C. The equivalent line for 5 kbar and 800 °C should lie at slightly higher $m/(1-m)$ values

Comparison with previous models and applications for fluid saturation in cordierite

Kurepin (1984) produced a model for the P–T dependence of CO₂ uptake in cordierite based at least in part on the Johannes and Schreyer (1981) data set. This model implies a double-link between $a\text{CO}_2$ and $m+n$, as the formulation for CO₂-cordierite/volatile-free-cordierite is given as $m/(1-m-n)$. However, even with this interdependence between m and n , the Kurepin (1984) model does not fit the data for either cordierite A or B of Johannes and Schreyer (1981) particularly well.

A comparison of our model with that of Kurepin (1984) at 5 kbar and 900 °C is shown in terms of molecules of CO₂ (m) versus molecules of H₂O (n) per formula unit in Fig. 6. The predicted volatile contents differ significantly at both the high-CO₂ and high-H₂O ends, in part because of the different end member saturation values used. In the H₂O system, n from Harley and Carrington (2001) is greater than the fit to Mirwald et al. (1979) used by Kurepin (1984). In contrast, m extrapolated from our 5-kbar, 900 °C data in H₂O–CO₂ (this work) is less than that modelled by Kurepin (1984) from the Johannes and Schreyer (1981) cordierite A data. The overall curvature of the saturation surface is greater in our model, with the Kurepin (1984) model yielding an almost linear relation of m to n that does not fit our measured m – n relationship (Fig. 6) nor the data of Johannes and Schreyer (1981) in detail. When considered in detail it is apparent that the formulation used by Kurepin (1984) is incorrect as it implicitly involves a coupling between m and n , and hence $a\text{CO}_2$ and $a\text{H}_2\text{O}$. This coupling does not exist if a free fluid phase is absent (i.e. in fluid absent conditions) or indeed if the H₂O–CO₂ fluid phase is diluted by other components that may or may not enter cordierite (e.g. N, Ar, dissolved species). The formulation used by Kurepin (1984) over-defines

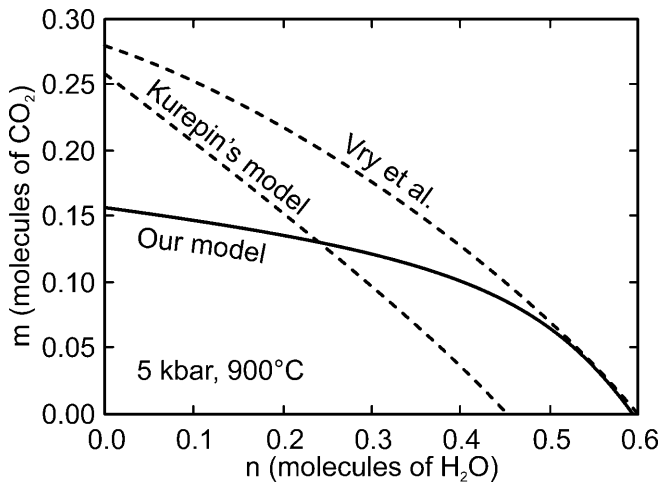


Fig. 6 A comparison of the co-variance of H₂O and CO₂ at fluid saturation for the models of Kurepin (1984), Vry et al. (1990) and the one proposed here

the system and hence is not appropriate for fluid activity calculations using cordierite H₂O–CO₂ contents.

The problems inherent in the Kurepin (1984) formulation are well illustrated by consideration of hypothetical fluid-undersaturated cordierites formed at 5 kbar and 900 °C with $n=0.3$. Using our formulation $[n/(1-n)]$, $a_{\text{H}_2\text{O}}$ is 0.29 and independent of the amount of CO₂ in the cordierite, which could vary in the range $0 \leq m < 0.13$ before fluid saturation is reached (Fig. 6). In contrast, in the Kurepin (1984) model, $a_{\text{H}_2\text{O}}$ increases as CO₂ is added to the cordierite, from 0.29 at $m=0$ to 0.323 at $m=0.08$, the saturation m value obtained for $n=0.3$ if the Kurepin (1984) $(1-m-n)$ denominator is used. This correlation between $a_{\text{H}_2\text{O}}$ and a_{CO_2} contravenes the phase rule as it implies that cordierites with two distinct values of n would define the same $a_{\text{H}_2\text{O}}$ at fixed P–T simply if their CO₂ contents were different. In short, the assumption of closure between anhydrous-cordierite, H₂O–cordierite and CO₂–cordierite inherent in the Kurepin (1984) model does not apply because cordierite can be volatile-undersaturated, as demonstrated conclusively by Carrington and Harley (1996). At saturation, the exchange reaction (3) ensures that as a_{CO_2} and m rise then $a_{\text{H}_2\text{O}}$ and n decrease for any specified P–T condition.

Vry et al. (1990) have also modelled the saturation H₂O–CO₂ contents of cordierite by combining selected experimental constraints including the H₂O-system data of Mirwald and Schreyer (1977) and Armbruster and Bloss (1980), the cordierite A H₂O–CO₂ results of Johannes and Schreyer (1981), and the CO₂-system cordierite results of Armbruster and Bloss (1982). The Vry et al. (1990) model uses the simplification that the percentage decreases in channel occupancy with XCO₂ (Crd) as modelled at 5 kbar and 600 °C are also applicable at all high-grade P–T conditions. This implicitly assumes that the isopleths of n (H₂O) and m (CO₂) in cordierite have both equal slopes and relative spacings in

P–T space, which unfortunately is not the case. Figure 6 shows a comparison of our model with that of Vry et al. (1990) at 5 kbar and 900 °C in terms of molecules of CO₂ (m) versus molecules of H₂O (n) per formula unit. In this comparison we have used our value of $n=0.6$ for the end point in the H₂O-system for Vry et al.'s model. Vry et al. compared models with different H₂O-system isopleths taken from a number of sources as illustrated on their Fig. 10. At 5 kbar, 900 °C these isopleths give approximate values of n of 0.42 (Helgeson et al. 1978), 0.55 (Mirwald et al. 1979) and 0.66 (Mirwald and Schreyer 1977; Armbruster and Bloss 1980). Vry et al.'s model and our model diverge progressively as XCO₂ (Crd) increases and n is reduced. The value of m extrapolated from our 5 kbar, 900 °C data in H₂O–CO₂ (0.16) is significantly less than that obtained using the approach of Vry et al. (1990: 0.28 molecules per formula unit.), which itself is even higher than that calculated using Kurepin (1984).

The net effect of the above comparisons is that, at 5 kbar and 900 °C, the saturation CO₂ content and H₂O–CO₂ contents of cordierite with high channel XCO₂ are lower than previously thought. This impacts upon the arguments put forward by Vry et al. (1990) to explain the apparently low total volatile contents, for specified P–T conditions of equilibration, of many of the cordierites reported in their study. Vry et al. (1990) considered that loss of volatiles during uplift and cooling was typical of most cordierites as their model suggested large volatile deficiencies for various cordierites from a range of environments. Such volatile leakage is no longer required to explain the volatile compositions of many of the CO₂-richer cordierites tabulated by Vry et al. (1990), although several examples of CO₂-poor cordierites are still volatile-deficient and hence imply some degree of volatile loss and/or equilibration under volatile-deficient conditions (Harley and Carrington, 2001). Whilst volatile leakage can explain the low channel volatile contents measured in some cordierites, it is clearly necessary to evaluate this for individual cases using the spatial resolution provided by SIMS to test for intra- and intergrain variability and zoning in H₂O and CO₂. Natural cordierite volatile content data can only be explicitly compared with the experimental cordierite data if the shifts of the modelled saturation curves, depicted in Figs. 4 and 6, with pressure and temperature, are taken into account (Harley et al. 2001).

A further key implication of the new experimental results is that our model predicts that fluid-saturated cordierites with channel XCO₂ > 0.25 imply a_{CO_2} of > 0.7 whereas the Kurepin (1984) and Vry et al. (1990) models yield lower a_{CO_2} , in the range 0.4–0.45 for the same channel XCO₂ (Fig. 7). A good example of this effect is provided by cordierite that coexists with calcite in a 'reaction rock' from Finmark, Norway, which preserves channel XCO₂ of 0.75 and is inferred to have been formed in equilibrium with a near-pure CO₂ fluid (Armbruster et al. 1982). If the a_{CO_2} –XCO₂ relations depicted on Fig. 7 are essentially independent of pres-

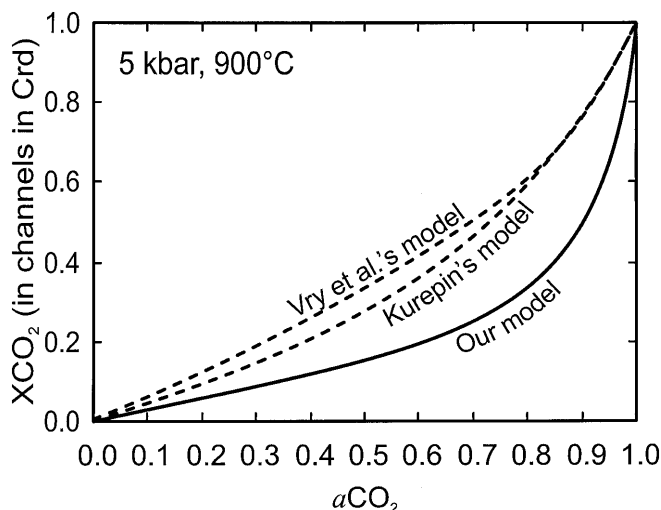


Fig. 7 The channel X_{CO_2} measured in a fluid-saturated cordierite would lead to a significant underestimate of the a_{CO_2} using either the model of Kurepin (1984) or Vry et al. (1990) in comparison to ours

sure and temperature, the a_{CO_2} for the Armbruster et al. rock is calculated as 0.96 using our calibration compared with 0.88 using the a - X relations of Kurepin and Vry et al.

Conclusions

The experimental data obtained here at 5 kbar and 900 °C demonstrate that the uptake of CO_2 by cordierite has a negligible effect on the distribution of H_2O between cordierite and coexisting melt (D_w) described by Harley and Carrington (2001). Incorporation of CO_2 into cordierite can be modelled simply by using a one-site formulation with a_{CO_2} being proportional to $m/(1-m)$, where m is the number of molecules of CO_2 per formula unit of cordierite, and does not follow the coupled H_2O - CO_2 model developed by Kurepin (1984) and subsequently applied by other workers. Most importantly, our self-consistent results show that the maximum CO_2 content of cordierite (i.e. at $a_{CO_2}=1$) is significantly less than previously modelled for the experimental conditions. As a consequence, volatile-saturation in CO_2 -bearing cordierites may be more common than previously inferred, and the a_{CO_2} of fluids associated with the equilibration of such cordierites may be greater than previously calculated for measured cordierite channel compositions.

The production of similar cordierite H_2O - CO_2 data for a variety of experimental conditions will ultimately allow the saturation CO_2 contents of cordierite to be modelled and evaluated over the range of P-T conditions of crustal metamorphism, and hence provide both a_{H_2O} and a_{CO_2} estimates from cordierites such as those considered here. Such polybaric-polythermal experimental data will be described and modelled in a

further paper that builds upon the analysis presented herein.

Acknowledgements This work has been supported by a UK Natural Environment Research Council grant GR3/9099 to S.L.H. We are grateful for the advice and assistance of Steve Elphick and Bob Brown (experimental apparatus), John Craven and Richard Hinton (SIMS analysis), Pete Hill and Simon Burgess (EMP analysis), and David Plant (SEM analysis). Standards were analysed by Tony Fallick, Francois Holtz, Dave Matthey and Volker Schenk. Dave Matthey evacuated our cordierite starting materials. We thank Werner Schreyer and Hanna Nekvasil for detailed and constructive reviews that greatly improved the clarity of this paper.

References

- Armbruster T, Bloss FD (1980) Channel CO_2 in cordierites. *Nature* 286:140-141
- Armbruster T, Bloss FD (1982) Orientation and effects of channel H_2O and CO_2 in cordierite. *Am Mineral* 67:284-291
- Armbruster T, Schreyer W, Hoefs J (1982) Very high CO_2 cordierite from Norwegian Lapland: mineralogy, petrology and carbon isotopes. *Contrib Mineral Petrol* 81:262-267
- Barbey P, Macaudiere J, Nzenti J (1990) High-pressure dehydration melting of metapelites. *J Petrol* 31:401-427
- Blank JG, Brooker RA (1994) Experimental studies of CO_2 in silicate melts: solubility, speciation and stable carbon isotope behaviour. *Rev Mineral* 30:157-186
- Boberski C, Schreyer W (1990) Synthesis and water contents of Fe^{2+} -cordierites. *Eur J Mineral* 2:565-584
- Burnham CW (1994) Development of the Burnham model for prediction of H_2O solubility in magmas. In: Carroll MR, Holloway JR (eds) Volatiles in magmas. *Mineral Soc Am, Rev Mineral* 30:123-129
- Burnham CW, Nekvasil H (1986) Equilibrium properties of granitic pegmatite magmas. *Am Mineral* 71:239-263
- Carey JW (1995) A thermodynamic formulation for hydrous cordierite. *Contrib Mineral Petrol* 119:155-165
- Carrington DP, Harley SL (1995) Partial melting and phase relations in high-grade metapelites: an experimental petrogenetic grid in the KFMASH system. *Contrib Mineral Petrol* 120:270-291
- Carrington DP, Harley SL (1996) Cordierite as a monitor of fluid and melt water contents in the lower crust: an experimental calibration. *Geology* 24:647-650
- Clemens JD (1993) Experimental evidence against CO_2 -promoted deep crustal melting. *Nature* 363:336-338
- Fogel RA, Rutherford MJ (1990) The solubility of CO_2 in rhyolitic melts: a quantitative FTIR study. *Am Mineral* 75:1311-1326
- Goldman DS, Rossman GR, Dollase WA (1977) Channel constituents in cordierite. *Am Mineral* 62:1144-1157
- Harley S (1994) Cordierite as a sensor of fluid and melt distribution in crustal metamorphism. *Mineral Mag* 58A:374-375
- Harley SL, Carrington DP (2001) The distribution of H_2O between cordierite and granitic melt: Improved calibration of H_2O incorporation in cordierite and its application to high-grade metamorphism and crustal anatexis. *J Petrol* (in press)
- Harley SL, Thompson P, Buick IS, Hensen BJ (2001) Cordierite as a sensor of high grade metamorphic processes. *J Metam Geol* (in press)
- Helgeson HC, Delany JM, Nesbitt HW, Bird DK (1978) Summary and critique of the thermodynamic properties of rock-forming minerals. *Am J Sci* 278A:1-229
- Holland TJB, Powell R (1990) An enlarged and updated internally consistent thermodynamic dataset with uncertainties and correlations: the system K_2O - Na_2O - CaO - MgO - MnO - FeO - Fe_2O_3 - Al_2O_3 - TiO_2 - SiO_2 - C - H_2O - O_2 . *J Metamorph Geol* 8:89-124
- Holloway JR, Blank JG (1994) Application of experimental results to C-O-H species in natural melts. *Rev Mineral* 30:187-230

- Holtz F, Johannes W (1994) Maximum and minimum water contents of granitic melts. *Lithos* 32:149–159
- Holtz F, Behrens H, Dingwell DB, Taylor RB (1992) Water solubility in aluminosilicate melts of haplogranite composition at 2 kbar. *Chem Geol* 96:289–302
- Johannes W, Holtz F (1996) Petrogenesis and experimental petrology of granitic rocks. Springer, Berlin Heidelberg New York
- Johannes W, Schreyer W (1981) Experimental introduction of CO₂ and H₂O into Mg-cordierite. *Am J Sci* 281:299–317
- Kurepin VA (1984) H₂O and CO₂ contents of cordierite as an indicator of thermodynamical conditions of formation. *Geokhimiya* 8:1125–1134
- Kurepin VA (1985) H₂O and CO₂ contents of cordierite as an indicator of thermodynamical conditions of formation. *Geochim Int* 22:148–156
- Le Breton N, Schreyer W (1993) Experimental CO₂ incorporation in Mg-cordierite: non-linear behaviour of the system. *Eur J Mineral* 5:427–438
- Mirwald PW, Schreyer W (1977) Die stabile und metastabile Abbaureaktion von Mg-cordierit in Talk, Disthen und Quarz und ihre Abhängigkeit vom Gleichgewichtswassergehalt des Cordierits. *Fortschr Mineral* 55:95–97
- Mirwald PW, Maresch WV, Schreyer W (1979) Der Wassergehalt von Mg-cordierit zwischen 500 °C und 800 °C sowie 0.5 und 11 kbar. *Fortschr Mineral* 57:101–102
- Mukhopadhyay B, Holdaway MJ (1994) Cordierite-garnet-sillimanite-quartz equilibrium: New experimental calibration in the system FeO-Al₂O₃-SiO₂-H₂O and certain P-T-XH₂O relations. *Contrib Mineral Petrol* 116:462–472
- Newton R, Smith J, Windley B (1980) Carbonic metamorphism, granulites, and crustal growth. *Nature* 288:45–49
- Papale P (1997) Thermodynamic modelling of the solubility of H₂O and CO₂ in silicate liquids. *Contrib Mineral Petrol* 126:237–251
- Petersen JW, Newton RC (1990) Experimental biotite-quartz melting in the KMASH-CO₂ system and the role of CO₂ in the petrogenesis of granites and related rocks. *Am Mineral* 75:1029–1042
- Santosh M, Harris NBW, Jackson DH, Matthey DP (1990) Dehydration and incipient charnockite formation: a phase equilibria and fluid inclusion study from south India. *J Geol* 98:915–926
- Schmulovich KI, Graham CM (1996) Melting of albite and dehydration of brucite in H₂O-NaCl fluids to 9 kbar and 700–900 °C: implications for partial melting and water activities during high pressure metamorphism. *Contrib Mineral Petrol* 124:370–382
- Schreyer W (1985) Experimental studies on cation substitutions and fluid incorporation in cordierite. *Bull Mineral* 108:273–291
- Skippen GB, Gunter AE (1996) The thermodynamic properties of H₂O in magnesian and iron cordierite. *Contrib Mineral Petrol* 124:82–89
- Stevens G, Clemens JD (1993) Fluid-absent melting and the roles of fluids in the lithosphere: a slanted summary? *Chem Geol* 108:1–17
- Stevens G, Clemens JD, Droop GTR (1995) Hydrous cordierite in granulites and crustal magma production. *Geology* 23:925–928
- Thompson P, Harley SL, Carrington DP (2001) Sodium and potassium in cordierite – a potential thermometer for melts? *Eur J Mineral* (in press)
- Vielzeuf D, Holloway JR (1988) Experimental determination of the fluid-absent melting relations in the pelitic system. Consequences for crustal differentiation. *Contrib Mineral Petrol* 98:257–276
- Vry JK, Brown P, Valley J (1990) Cordierite volatile content and the role of CO₂ in high-grade metamorphism. *Am Mineral* 75:71–88
- Waters DJ, Whales D (1984) Dehydration melting and the granulite transition in metapelites from southern Namaqualand, S. Africa. *Contrib Mineral Petrol* 88:269–275
- Watt GR, Harley SL (1993) Accessory phase controls on the geochemistry of crustal melts and restites produced by dehydration melting. *Contrib Mineral Petrol* 114:550–566